



Article

# Boosting the Lithium Storage Properties of a Flexible Li<sub>4</sub>Ti<sub>5</sub>O<sub>12</sub>/Graphene Fiber Anode via a 3D Printing Assembly Strategy

Chenpeng Zhao, Rui Wang, Biao Fang, Han Liang, Biyuan Nie, Ruyi Wang, Biao Xu, Songyang Feng, Ruqing Li, Shuaifei Li, Yuhui Xiong, Yuye Shao and Runwei Mo \*

School of Mechanical and Power Engineering, East China University of Science and Technology, Shanghai 200030, China; y84210016@mail.ecust.edu.cn (C.Z.)

\* Correspondence: rwmo@ecust.edu.cn

**Abstract:** Traditional lithium-ion batteries cannot meet the high flexibility and bendability requirements of modern flexible electronic devices due to the limitations of the electrode material. Therefore, the development of high-performance flexible energy storage devices is of great significance for promoting flexible electronics. In recent years, one-dimensional flexible fiber lithium-ion batteries have been rapidly developed due to their advantages of high flexibility and bendability. However, it remains highly challenging to realize 1D flexible fiber lithium-ion batteries with excellent electrochemical properties and good mechanical performance. In this work, a reduced graphene oxide-based printing ink is proposed for the fabrication of flexible Li<sub>4</sub>Ti<sub>5</sub>O<sub>12</sub>/graphene fiber electrodes using a 3D printing assembly strategy. It is noteworthy that the green reducing agent vitamin C was used to reduce the graphene oxide in one step, which improved the conductivity of the fiber electrode. Furthermore, a 3D conductive network was constructed inside the fiber electrodes due to the high specific surface area of the reduced graphene oxide, which enhanced the electronic conductivity and ion mobility. The fiber electrode not only exhibits good mechanical performance, but also has excellent electrochemical properties. Equally importantly, the method is simple and efficient, and the working environment is flexible. It can precisely control the shape, size and structure of the one-dimensional fiber flexible electrode, which is of great significance for the development of future flexible electronic devices.

**Keywords:** 3D printing assembly strategy; flexible energy storage devices; fiber electrodes



**Citation:** Zhao, C.; Wang, R.; Fang, B.; Liang, H.; Nie, B.; Wang, R.; Xu, B.; Feng, S.; Li, R.; Li, S.; et al. Boosting the Lithium Storage Properties of a Flexible Li<sub>4</sub>Ti<sub>5</sub>O<sub>12</sub>/Graphene Fiber Anode via a 3D Printing Assembly Strategy. *Batteries* **2023**, *9*, 493. <https://doi.org/10.3390/batteries9100493>

Academic Editor: Elod Gyenge

Received: 18 August 2023

Revised: 18 September 2023

Accepted: 22 September 2023

Published: 27 September 2023



**Copyright:** © 2023 by the authors. Licensee MDPI, Basel, Switzerland. This article is an open access article distributed under the terms and conditions of the Creative Commons Attribution (CC BY) license (<https://creativecommons.org/licenses/by/4.0/>).

## 1. Introduction

With the rapid development of science and technology, people are increasingly interested in emerging technologies such as wearable devices, flexible smart electronics, and flexible electronic devices. These technologies represent the future development direction of the electronics industry and will bring a more convenient and intelligent experience to people's lives [1]. In particular, compared with traditional rigid electronic devices, flexible electronic devices have obvious advantages in terms of adapting to complex environments, body curves, and various daily uses [2]. Such devices are suitable for use not only in personal wearable devices such as smart watches, smart glasses, and smart clothing, but also in smart homes, medical monitoring, and environmental monitoring, bringing new experiences to people's lives [3]. However, there are many challenges in making flexible electronic devices work well under frequent bending and stretching deformation conditions. Since the working environment of flexible electronic devices often requires electronic components to be able to bend, stretch, and deform, this places high demands on the materials used in electronic devices [4]. Traditional rigid materials have difficulty adapting to such frequent deformation working conditions, and they are prone to damage and fatigue. Therefore, in order to produce reliable flexible electronic devices, researchers are

continuing to explore various new flexible materials to improve the durability and stability of these devices. First, focusing on the limitations of traditional materials, researchers have developed a series of new materials with good flexibility and bendability. For example, polymer materials are widely used in the field of flexible electronics. Due to their plasticity and high toughness, the electronic components can maintain the excellent performance when bent and stretched [5]. In addition, nanomaterials such as carbon nanotubes and two-dimensional materials have also been introduced into flexible electronic devices, and their excellent mechanical and electrical properties provide strong support for the stable operation of the devices [6–10].

Lithium-ion batteries, a new type of battery that has undergone rapid development in recent years, are leading the revolution in the field of energy storage due to their excellent performance characteristics. First, the high energy density of lithium-ion batteries makes them the energy source of choice for portable electronic devices. With the popularity of mobile communications, smart phones, tablets, and other portable devices, people's requirements for battery capacity and endurance are increasingly high [11]. Lithium-ion batteries are able to store more energy in a relatively small space, thus extending the usage time of the device and providing a more convenient user experience. At the same time, the long lifecycle of lithium-ion batteries makes them excellent in long-term usage scenarios such as medical monitoring. Medical devices and monitoring equipment often require a long-term continuous power supply, and lithium-ion batteries can maintain relatively stable performance after thousands of charge and discharge cycles, providing reliable energy support for these applications; in the case of non-use, lithium-ion batteries exhibit less energy loss, can maintain the state of the stored energy for a long time, and enable the convenient storage of energy [12].

In recent years, traditional lithium-ion batteries have achieved great success in the field of energy storage. However, there are still some serious problems and limitations regarding the special requirements of flexibility and bendability. These problems mainly involve electrode materials, manufacturing processes, and packaging technologies, which limit the development of traditional lithium-ion batteries in flexible applications. First of all, the rigidity of the electrode material is not able to adapt to the deformation requirements of flexible electronic devices. The electrode materials of traditional lithium-ion batteries are usually composed of rigid materials such as metal foils and ceramic films, which are prone to cracks, fractures, and even delamination during frequent bending, stretching, and deformation [13]. The rigidity of this material limits the stability and life of the battery in its bent state, making it difficult for the battery to work continuously and stably in a flexible environment. Second, the traditional manufacturing process has difficulty adapting to the production needs of flexible batteries. The manufacturing of traditional lithium-ion batteries usually involves coating and other processes, and the application of these processes to flexible substrates is significantly limited. These processes not only damage the flexible base material but can also lead to separation between the electrode material and the electrolyte, which can affect the performance and stability of the battery [14]. In addition, packaging technology is also a key issue that restricts the flexibility of traditional lithium-ion batteries. Because the battery needs to maintain a stable internal environment during use, traditional packaging methods are often unable to meet the requirements of flexible battery deformation. Bending and stretching can cause damage to the packaging layer, making the inside of the battery vulnerable to the external environment, which affects the performance and life of the battery. Most importantly, frequent deformation can cause problems with the interface between the various functional components inside the battery. Components such as electrode materials, electrolytes, and diaphragms inside the battery are prone to slight displacement and stress concentration during deformation, which may lead to fatigue damage and the formation of defects at the interface. This interface failure leads to instability in the battery's performance, and it can even cause local failure, which seriously affects the reliability and service life of the battery [15]. To sum up, traditional lithium-ion batteries encounter a series of problems in terms of flexibility and bendability,

mainly involving the rigidity of electrode materials, manufacturing process limitations, and challenges in packaging technology. These problems not only restrict the development of flexible electronic devices, but also limit the widespread promotion of flexible batteries in practical applications. In order to overcome these problems, it is necessary to innovate in material research, manufacturing processes, and packaging technology to achieve the reliability and stability of flexible lithium-ion batteries and to promote the application of flexible electronic technology in more fields.

In recent years, one-dimensional (1D) flexible fiber-optic lithium-ion batteries have undergone rapid development due to their high flexibility and bendability. This unique design concept integrates fiber electrode materials and flexible electrolytes, not only bringing together the advantages of traditional lithium-ion batteries, but also integrating multiple characteristics such as flexibility, plasticity, and electrical conductivity. This innovative combination creates new prospects for the field of electronic technology, potentially triggering a revolutionary change in the field of electronic devices. The unique feature of the one-dimensional flexible fiber-optic lithium-ion batteries is that they can be bent and twisted freely to adapt to the needs of various application scenarios. This gives the batteries excellent flexibility, weaving abilities, and wearability, meaning that they have a wide range of applications in smart textiles, wearable devices, medical monitoring, and other fields. On the one hand, the high degree of plasticity of these batteries allows them to respond flexibly in a variety of complex environments, providing greater freedom for the design and use of electronic devices. On the other hand, it provides convenient energy solutions for areas such as smart textiles, creating entirely new possibilities for the development of these areas [16–20]. Compared with 2D and 3D flexible electrodes, 1D flexible fiber electrodes allow for a larger bending range and better stretchability, exhibiting better flexibility in flexible electronics [21]. For example, Cai integrated fiber electrodes into a wristwatch, harnessing their mechanical robustness to enable the watch to maintain an electrical energy supply even when fully bent [22]. This innovation eliminates the need for frequent battery replacements, enhancing the convenience and sustainability of use. Similarly, Park and colleagues integrated fiber capacitors into flexible smart contact lenses [23]. These lenses boast excellent stretch durability and comfort. Furthermore, following wireless charging, their flexible fiber capacitors can illuminate LEDs on the lenses. These smart contact lenses have the potential to be used for collecting eye data, displaying health information, or providing augmented reality experiences while maintaining comfort, offering innovative solutions for the fields of medical monitoring and entertainment. However, significant challenges remain in the fabrication of 1D fiber flexible electrodes. Traditional 1D flexible fiber electrodes usually require complex fabrication techniques and conditions, such as electrospinning [24,25], chemical vapor deposition [26], sol–gel [27], etc. These manufacturing technologies have high requirements in terms of special equipment and environments, which greatly increases the complexity and cost of the manufacturing process. These complex process requirements mean that more resources and effort need to be invested, including specific equipment and controlled production environments, thus limiting the scale production of one-dimensional flexible fiber electrodes and the possibility of their widespread application [13]. In addition, in order to obtain the advanced mechanical properties required for fiber electrodes, it is usually necessary to introduce a large number of polymer binders into the fiber structure, which ensures the structural stability of the fiber to a certain extent. However, this added polymer binder often has a negative impact on the electrochemical performance of the electrode, including a reduction in conductivity and a loss of capacity, which affects the overall performance of the battery. In contrast, in order to pursue excellent electrochemical performance, a large number of conductive materials are sometimes added to the fiber electrode to improve the energy density and power density of the battery. However, this practice often comes at the expense of the mechanical properties of the fiber electrode, making it brittle and prone to breakage. This trade-off is a complex challenge that requires finding a balance in the design and preparation of the fiber electrode in order to achieve adequate mechanical stability without compromising electrochemical

performance [28,29]. Therefore, it remains challenging to achieve both excellent electrochemical performance and effective mechanical properties in one-dimensional flexible fiber lithium-ion batteries; it is a task that requires the careful design of the structure and composition of the fiber electrode, as well as the optimization of the interaction between the materials to overcome the limitations of existing technologies. Such achievements will push flexible battery technology to the next level, providing more reliable and efficient energy solutions for wearables, smart textiles, and other mobile power applications.

As an emerging material processing technology, 3D printing is leading the gradual innovation and development of the manufacturing field with its unique characteristics. The technology has a series of advantages, such as simple operations and a flexible working environment, in addition to flexible material selection, allowing for the use of a variety of different materials, including polymers [30], metals [31] and other materials. This not only changes the traditional manufacturing method, but also brings greater flexibility and innovation to a number of fields [32–35]. Direct ink writing (DIW) printing is a typical extrusion deposition 3D printing technology, and its operation is relatively simple and efficient. The core principle of this method is that it uses a nozzle or needle to extrude material in the form of a viscous ink or glue, layer by layer, to build the desired three-dimensional structure. One of the reasons why this technology is so popular is its material mix flexibility, which allows many different types of materials to be mixed to suit different application needs [36]. Moreover, DIW technology also performs well in enabling high-precision repetitive manufacturing. Through careful control and adjustment, the diameter, spacing, and arrangement of the fibers can be precisely controlled. This high degree of consistency facilitates the fabrication of fiber electrodes with the same shape, size, and electrochemical properties in different manufacturing batches. This is important for applications that require large-scale manufacturing and consistency [37,38]. In addition, compared with traditional manufacturing methods, DIW technology has brought significant advantages in terms of material use and manufacturing costs, bringing revolutionary changes to the manufacturing industry. Traditional manufacturing methods usually require a large amount of raw material to make products, some of which may be discarded due to waste during processing. However, DIW technology, with its unique working principle, is able to accurately transform materials into the desired structure, with almost no material waste problems. This helps relieve the pressure of excessive resource consumption. Second, generally, DIW technology does not require high temperatures or large-scale industrial equipment, so it has relatively low energy consumption. This helps reduce carbon emissions during manufacturing. Moreover, some printing materials are recyclable, which helps reduce material waste and reduces reliance on natural resources. At the same time, DIW technology does not require custom molds and a lot of human input, and additional costs in the manufacturing process can be reduced, improving production efficiency and cost effectiveness [39].

In this work, a reduced graphene-oxide-based printing ink is proposed to fabricate flexible  $\text{Li}_4\text{Ti}_5\text{O}_{12}$ /graphene fiber electrodes via a 3D printing assembly strategy. Specifically, an ink for 3D printing was synthesized, in which lithium titanate (LTO) was added as the active material, polyvinylidene fluoride (PVDF) was used as a binder to enhance the mechanical properties of the fiber electrodes, and graphene oxide (GO) acted as a conductive agent. It is worth noting that PVDF and GO have good biocompatibility [40–42], and LTO also has low toxicity [43,44], so this fiber electrode has wide application potential. As a new type of carbon material, GO is relatively simple to manufacture and low in cost, thus meeting the needs of large-scale manufacturing through mass production [45]. Additionally, it has a larger specific surface area [46,47], which increases the loading of active materials and improves the electrochemical performance. At the same time, GO has good solubility in water and organic solvents [48], which is convenient for fabrication and processing into electrodes of different shapes and sizes. However, GO has the disadvantages of relatively low electrical conductivity and poor electrochemical stability [49]. In order to improve the material's electrical conductivity and electrochemical stability, the green reducing agent vitamin C was used to reduce graphene oxide in one step [50]. It is worth noting that,

compared with GO, the reduced graphene oxide (rGO) exhibits higher electrical conductivity [51–55] and mechanical properties [56,57], which is mainly attributed to the removal of oxidized functional groups. Furthermore, a 3D conductive network is constructed inside the fiber electrodes due to the high specific surface area of reduced graphene oxide, which enhances the electronic conductivity and ion mobility. The fiber electrode not only has good mechanical performance but also possesses excellent electrochemical properties. The elongation at break of the as-prepared one-dimensional fiber electrode was 35%, and the capacity retention rate of the one-dimensional fiber electrode was 83% after 100 cycles at 1C. This work is highly significant in terms of its potential impact on the further development and application of flexible fiber electrodes.

## 2. Materials and Methods

Shown in Figure 1 is the fabrication of the flexible  $\text{Li}_4\text{Ti}_5\text{O}_{12}$ /graphene fiber electrode (see the supporting information for detailed experimental procedures). In the printing ink,  $\text{Li}_4\text{Ti}_5\text{O}_{12}$  (LTO) is selected as the electrode active material, PVDF is used as the binder, vitamin C is used as the reducing agent, and rGO, obtained by reducing GO, is used as the conductive agent. After that, the printing ink is squeezed into deionized water through the nozzle of the 3D printer. The deionized water exchanges the solvent with NMP in the ink to precipitate PVDF in the ink, forming a fiber electrode. After passing through the PVDF-HFP solution, a separator is formed on the surface of the fiber electrode, which allows ions to pass through and prevents electrons from passing through. Finally, after drying at room temperature, the flexible  $\text{Li}_4\text{Ti}_5\text{O}_{12}$ /graphene fiber electrode can be prepared.

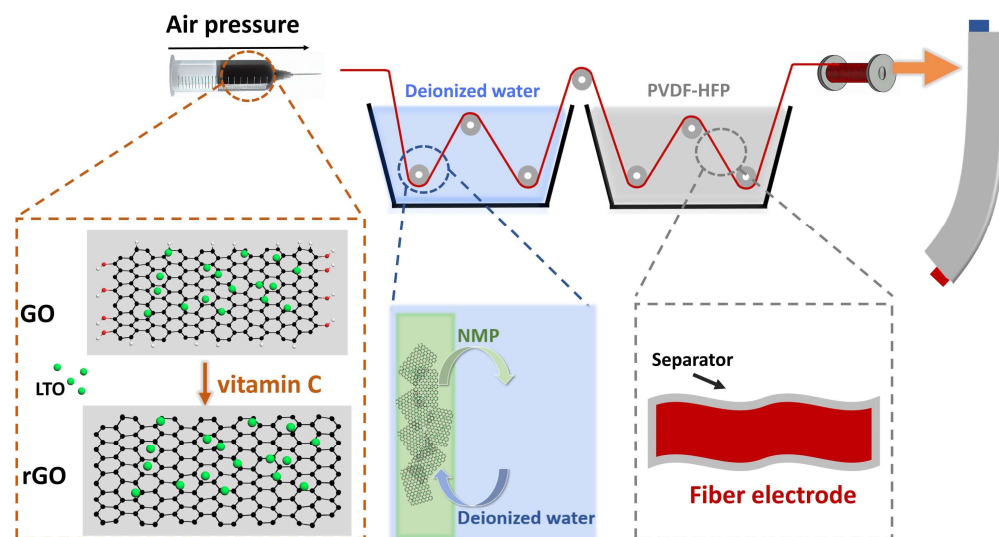


**Figure 1.** Schematic diagram of the flexible  $\text{Li}_4\text{Ti}_5\text{O}_{12}$ /graphene fiber electrode.

## 3. Results and Discussion

To make uniform fiber electrodes using a 3D printing assembly strategy, it is necessary to study the rheological properties of the printing ink. As shown in Figure 2a, the printing ink has an apparent viscosity of 3500 Pa s at a low shear rate ( $0.01 \text{ s}^{-1}$ ), and the apparent viscosity gradually decreases with the increase in the shear rate, which is consistent with the rheological behavior of non-Newtonian fluids [58]. This is the prerequisite for 3D printing to be carried out smoothly. This rheological property means that, during the 3D printing process, the viscosity of the printing ink can adapt to different shear rates, thus ensuring that the desired fluid flow can be achieved at different printing stages. Printing inks with good rheology enable precise material positioning and distribution when fabricating fiber electrodes, which facilitates electrode uniformity and consistency [59,60]. The excellent rheological properties enable the manufacturing speed of the fiber electrode to reach  $6 \text{ m min}^{-1}$ . Figure 2b shows that the fiber electrode has excellent deformation properties,

high flexibility, and bendability. The excellent deformation properties provide a wide range of possibilities for the application of electrodes in flexible electronic devices. They can adapt to the design requirements of various shapes and curves, and will not break or be damaged during the bending process. This flexibility and bendability provide a solid foundation for the practical application of fiber electrodes in wearable devices, smart textiles, and other fields. Tensile strength tests (Figure 2c) show that the prepared fiber electrode has up to 35% elongation at break, which means that the electrode can withstand tension to a certain extent, without breaking immediately when subjected to external forces. This high elongation at break is one of the most important advantages of fiber electrode materials, enabling the electrode to show excellent toughness and adaptability under strain and deformation. Figure 2d shows the difference in conductivity between GO and rGO. The conductivity of rGO reduced by vitamin C is  $10^3$  times higher than that of GO. The good electrical conductivity makes the fiber electrode form a high-speed electron transfer channel, which endows the fiber electrode with excellent electrochemical performance. In addition, the Raman spectrum (Figure 2f) shows the increase in the  $I_D/I_G$  of rGO compared to GO (Figure S1); this may be due to the reduction reaction forming smaller sized  $sp^2$  domains/rGO in larger quantities or the increased fraction of graphene edges [61]. From the XRD pattern (Figure 2e), it is clear that the main diffraction peak of LTO is very sharp, and there is no other impurity diffraction except for a broad and low-intensity carbon diffraction peak at  $2\theta$  of  $26^\circ$ – $27^\circ$ . This shows that the LTO/rGO fiber electrode prepared by 3D printing has no effect on the crystal structure of LTO, and does not introduce other impurities. Thermogravimetric analysis was performed on the fiber electrode in an oxygen atmosphere. As shown in Figure S2, PVDF in the fiber electrode decomposed at  $400^\circ\text{C}$ , and rGO decomposed at  $450^\circ\text{C}$ . According to the mass proportion of thermal decomposition, the material of the fiber electrode is evenly distributed in the electrode.

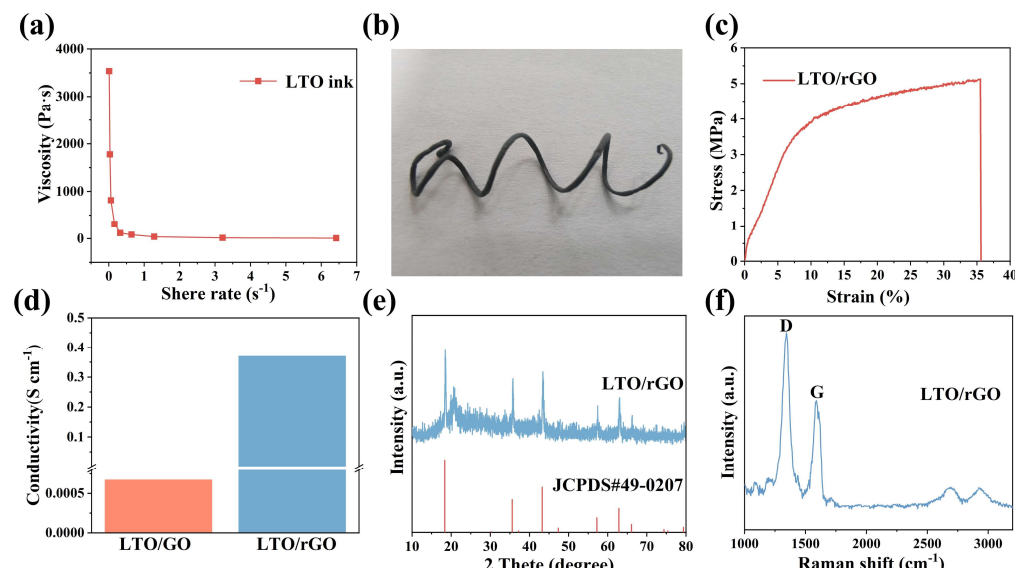


**Figure 2.** (a) Apparent viscosity of printing ink as a function of the shear rate; (b) LTO/rGO fiber electrode after drying; (c) tensile strength curve of LTO/rGO fiber electrode; (d) conductivity of LTO/GO and LTO/rGO; (e) XRD pattern of LTO/rGO fiber electrode; (f) Raman pattern of LTO/rGO fiber electrode.

The microscopic morphology of the LTO/rGO fiber electrode was observed using a scanning electron microscope (SEM). The surface microscopic morphology (Figure 3a–c) indicated that there are many small micropores on the surface of the electrode. The analysis revealed that the NMP inside the ink spontaneously flowed to the deionized water during the solvent exchange process, which resulted in the formation of tiny three-dimensional pore structures throughout the fiber electrodes. It is worth noting that this facilitates

the adsorption of electrolytes by the fibrous electrodes and the transport of ions during electrochemical processes [62]. The cross-sectional microstructure (Figure 3d–f) shows that the solvent will gradually migrate out of the electrode material under the surface tension of the solvent exchange. This process helps the structure of the fiber electrode to gradually become tighter, making the material denser. In this way, the internal void of the fiber electrode is effectively reduced, resulting in a more compact structure. This relatively dense structure has an important effect on the electrode's performance. First, the tighter structure can provide more contact points and conductive paths, which are conducive to the conduction of electrons and ions. Second, by reducing the internal void, the electrode's material is more closely in contact with the electrolyte, thus promoting the interaction between the electrode material and the electrolyte. This is highly significant for the charging and discharging process of the electrode, which can accelerate the reaction rate and improve the electrochemical performance of the electrode. As shown in Figure 3g, the size of the fiber electrode is 530  $\mu\text{m}$ , which is much smaller than the nozzle diameter of 650  $\mu\text{m}$ . The densified fiber electrode optimizes the ion conduction channel and speeds up the charge–discharge reaction rate. Moreover, rGO and LTO are uniformly dispersed inside, and LTO is located on the rGO sheet. Since rGO has many microscopic pores and a highly porous structure, the dispersion of LTO on its surface can make better use of these characteristics of rGO. This design not only increases the reaction interface between the electrode material and the electrolyte, but also provides more active sites, thus promoting the electrochemical reaction. The high specific surface area and good electrical conductivity of rGO allow electrons and ions to be transported more efficiently, thus improving the response speed and energy storage performance of the electrode [63]. Figure 3h shows that, after wetting with the PVDF–HFP solution, the thin film on the surface of the fiber electrode acts as a separator. This layer of the diaphragm plays a role in separating the electrode and the electrolyte during the operation of the battery, so that the electrolyte can evenly penetrate the inside of the electrode. This osmosis helps maintain ionic conductivity inside the battery, which helps to maintain a good connection between the electrode material and the electrolyte. The presence of the separator can also reduce the direct contact of electrode materials with the electrolyte inside the battery, helping to prevent unnecessary chemical reactions and protecting the stability and consistency within the battery. The diaphragm can also prevent the dissolution or corrosion of the electrode material and improve the cycle life and stability of the battery [64]. The EDS images (Figure 3i–l) show that the individual elements in the LTO/rGO fiber electrode are evenly distributed, which indicates that the 3D printing process, solvent exchange, drying, and other processes have no effect on the dispersion of the material.

As shown in Figure 4a, the discharge-specific capacity and charge-specific capacity of the LTO/rGO fiber electrode in the first cycle at the 1C rate are 182.8  $\text{mAh g}^{-1}$  and 173.2  $\text{mAh g}^{-1}$ , respectively; these values are close to the theoretical capacity of LTO (175  $\text{mAh g}^{-1}$ ). It is worth noting that the specific discharge capacity is higher than the theoretical value, which is mainly due to the contribution of rGO to the capacity [65]. The irreversible capacity loss is mainly attributed to the side reaction of LTO with the electrolyte and the formation of the SEI film [66,67]. The charge–discharge curves of the 50 cycles almost overlap, which indicates that the charge–discharge specific capacity is relatively stable. Figure 4b shows that a pair of reversible redox peaks are found at ~1.45 V and ~1.7 V, which are typical characteristic peaks of two-phase-reaction lithium titanate materials. This corresponds to the process of lithium intercalation/deintercalation in LTO [1]. Moreover, it can also be seen that each curve has a high degree of overlap and similar redox peaks, which indicates that the LTO/rGO fiber electrode has a good degree of reversibility. As shown in Figure 4d, the LTO/rGO fiber electrode exhibits excellent cycling stability. After 100 cycles, the specific discharge capacity and specific charge capacity of the LTO/rGO fiber electrode are 138.2  $\text{mAh g}^{-1}$  and 137.8  $\text{mAh g}^{-1}$ , respectively, and the capacity retention rate of the LTO/rGO fiber electrode can reach 83%. According to electrochemical impedance spectroscopy (Figure 4c), it can be concluded that, after

100 cycles, the impedance of the LTO/rGO fiber electrode increases, resulting in a decrease in the charge–discharge specific capacity. In addition, the LTO/rGO fiber electrode also exhibits outstanding rate performance, as shown in Figure 4e. The rate measurements deliver the capacities of 191.5, 175.3, 164.4, 156.2, and 127.2 mAh g<sup>−1</sup> at the rates of 0.1, 0.2, 0.5, 1 and 2 C, respectively. When the rate returns to 0.1 C, the capacity may still return to the original value. The excellent cycle performance and rate performance indicate that the LTO/rGO fiber electrode has high ionic conductivity and good electron transport abilities, which are mainly attributed to the three-dimensional channel structure formed by the solvent exchange on the surface of the fiber electrode. This facilitates the enhanced ion transport rate, as well as the electron conducting network formed in the fibrous electrodes.

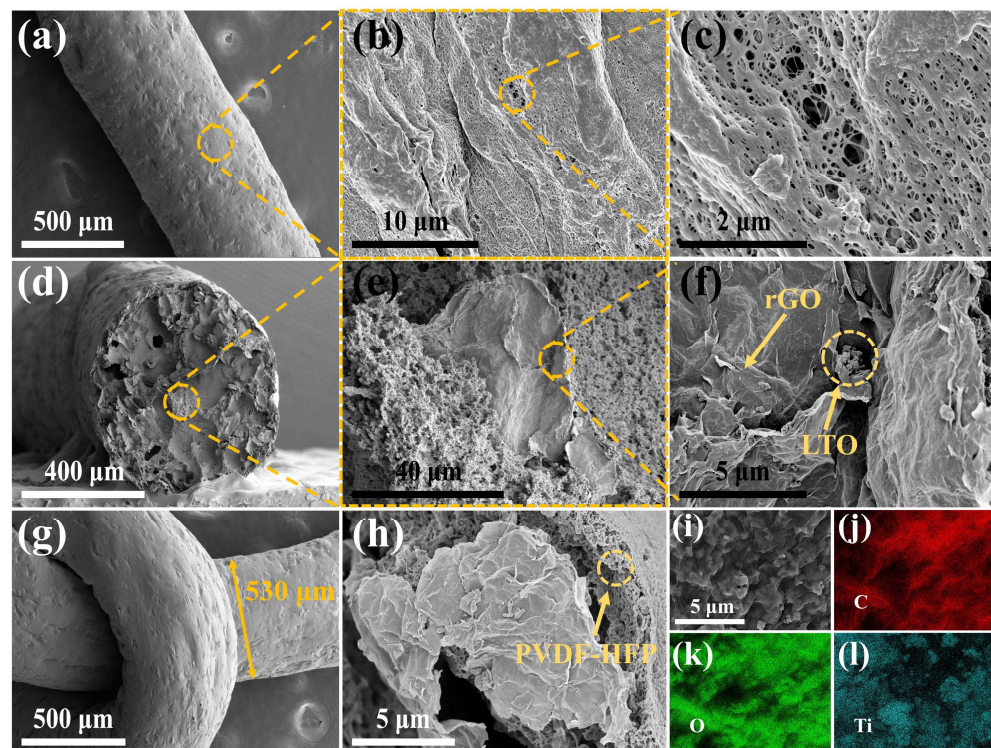


**Figure 3.** (a–c) Surface SEM image of the LTO/rGO fiber electrode; (d–f) cross-sectional SEM image of the LTO/rGO fiber electrode; (g) SEM image of the twisted LTO/rGO fiber electrode; (h) cross-sectional SEM image of the PVDF–HFP coating on the surface of the LTO/rGO fiber electrode; (i–l) EDS mapping of C, O, and Ti in LTO/rGO fiber electrodes.

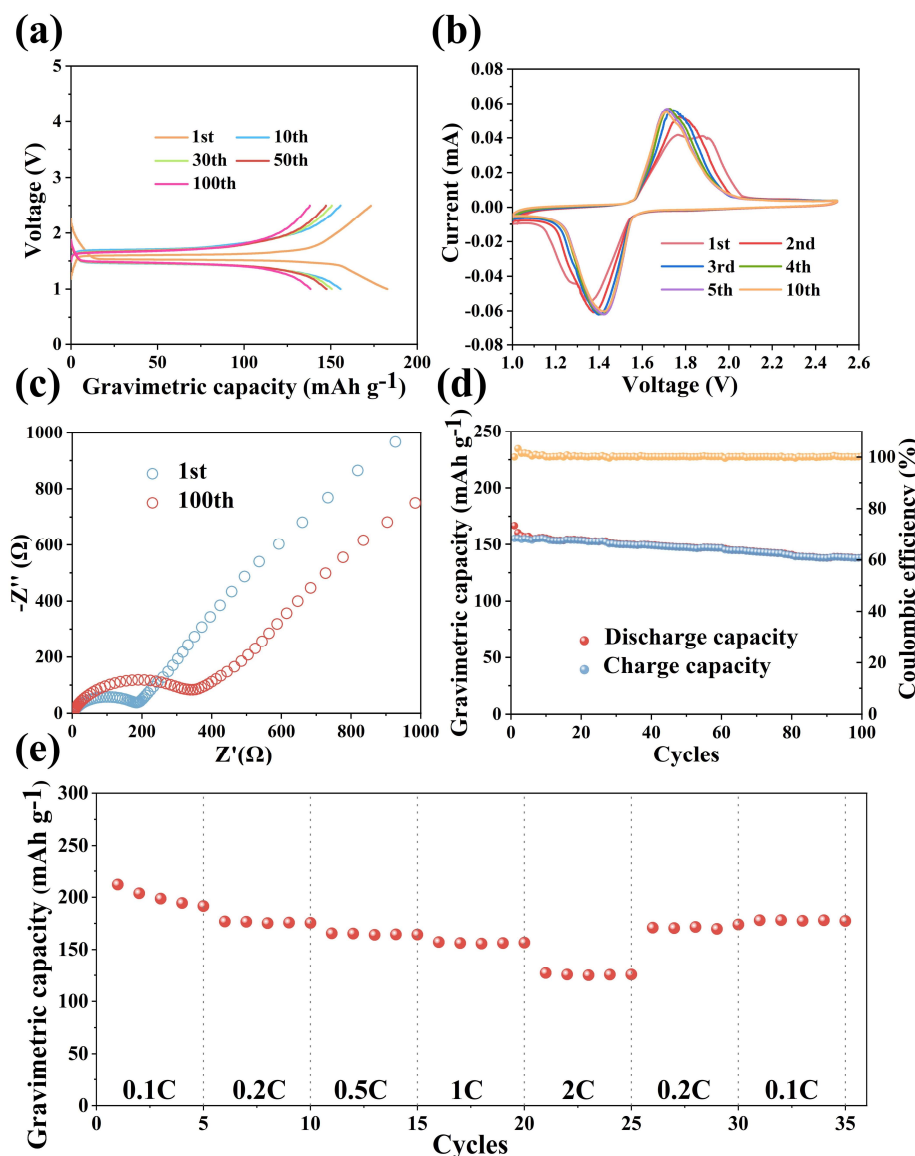


**Figure 4.** (a) Charge–discharge curves of LTO/rGO fiber electrodes at 1C current density; (b) CV curves of LTO/rGO fiber electrodes; (c) electrochemical impedance spectroscopy of the LTO/rGO fiber electrodes; (d) cycling performance of the LTO/rGO fiber electrode; (e) performance of LTO/rGO fiber electrodes at different current densities.

#### 4. Conclusions

In summary, we successfully prepared a flexible  $\text{Li}_4\text{Ti}_5\text{O}_{12}$ /graphene fiber electrode with a one-dimensional structure by configuring reduced graphene-oxide-based ink combined with extrusion 3D printing technology. Due to the high conductivity and high specific surface area of rGO, a 3D conductive network was constructed inside the fiber electrode, which improved the electronic conductivity. Furthermore, under the unique solvent exchange action, a tiny three-dimensional pore structure was formed on the surface of the fiber, which is conducive to the adsorption of electrolytes and the transmission of ions. The as-prepared fiber electrode not only exhibits excellent mechanical properties (35% elongation at break), but also exhibits outstanding electrochemical performance (83% capacity retention after 100 cycles). The method used to prepare the flexible fiber electrodes in this work is simple, environmentally friendly, and enables mass production, meaning that it has broad application prospects. More importantly, this preparation method can be

adapted to various deformable structures, which generates new possibilities in areas such as wearable electronics, flexible electronics, and implantable medical devices.

**Supplementary Materials:** The following supporting information can be downloaded at: <https://www.mdpi.com/article/10.3390/batteries9100493/s1>, Figure S1: Raman pattern of the LTO/GO fiber electrode; Figure S2: Thermogravimetric analysis of LTO/GO fiber electrodes.

**Author Contributions:** R.M. and C.Z., conceptualization; R.M., R.W. (Rui Wang), B.F., H.L., B.N., R.W. (Ruyi Wang), B.X., S.F., R.L., S.L., Y.X., Y.S. and C.Z., material synthesis, characterization, and electrochemical characterization; R.M., R.W. (Rui Wang), B.F., H.L. and C.Z., writing—original draft preparation, review, and editing. All authors have read and agreed to the published version of the manuscript.

**Funding:** This research was supported by the Shanghai pilotProgram for Basic Research (grant No. 22TQ1400100-8), the Shanghai Pujiang Program (grant No. 20PJ1402500), the Natural Science Foundation of Shanghai (grant No. 22ZR1416600), and the Fundamental Research Funds for the Central Universities.

**Data Availability Statement:** Data is unavailable due to privacy.

**Conflicts of Interest:** The authors declare no conflict of interest.

## References

- Shi, X.-L.; Chen, W.-Y.; Zhang, T.; Zou, J.; Chen, Z.-G. Fiber-based thermoelectrics for solid, portable, and wearable electronics. *Energy Environ. Sci.* **2021**, *14*, 729–764. [[CrossRef](#)]
- Tu, J.; Torrente-Rodríguez, R.M.; Wang, M.; Gao, W. The era of digital health: A review of portable and wearable affinity biosensors. *Adv. Funct. Mater.* **2020**, *30*, 1906713. [[CrossRef](#)]
- Rahman, M.T.; Rana, S.S.; Salauddin, M.; Maharjan, P.; Bhatta, T.; Park, J.Y. Biomechanical energy-driven hybridized generator as a universal portable power source for smart/wearable electronics. *Adv. Energy Mater.* **2020**, *10*, 1903663. [[CrossRef](#)]
- Chen, X. Making electrodes stretchable. *Small Methods* **2017**, *1*, 1600029. [[CrossRef](#)]
- Lv, Z.; Li, W.; Yang, L.; Loh, X.J.; Chen, X. Custom-made electrochemical energy storage devices. *ACS Energy Lett.* **2019**, *4*, 606–614. [[CrossRef](#)]
- Song, W.-J.; Lee, S.; Song, G.; Park, S. Stretchable aqueous batteries: Progress and prospects. *ACS Energy Lett.* **2019**, *4*, 177–186. [[CrossRef](#)]
- Song, Z.; Ma, T.; Tang, R.; Cheng, Q.; Wang, X.; Krishnaraju, D.; Panat, R.; Chan, C.K.; Yu, H.; Jiang, H. Origami lithium-ion batteries. *Nat. Commun.* **2014**, *5*, 3140. [[CrossRef](#)]
- Bao, Y.; Zhang, X.; Zhang, X.; Yang, L.; Zhang, X.; Chen, H.; Yang, M.; Fang, D. Free-standing and flexible LiMnTiO<sub>4</sub>/carbon nanotube cathodes for high performance lithium ion batteries. *J. Power Sources* **2016**, *321*, 120–125. [[CrossRef](#)]
- Fu, K.K.; Cheng, J.; Li, T.; Hu, L. Flexible batteries: From mechanics to devices. *ACS Energy Lett.* **2016**, *1*, 1065–1079. [[CrossRef](#)]
- Bao, Y.; Hong, G.; Chen, Y.; Chen, J.; Chen, H.; Song, W.-L.; Fang, D. Customized kirigami electrodes for flexible and deformable lithium-ion batteries. *ACS Appl. Mater. Interfaces* **2020**, *12*, 780–788. [[CrossRef](#)]
- Li, J.; Zhao, J.; Rogers, J.A. Materials and designs for power supply systems in skin-interfaced electronics. *Acc. Chem. Res.* **2019**, *52*, 53–62. [[CrossRef](#)] [[PubMed](#)]
- Armand, M.; Tarascon, J.-M. Building better batteries. *Nature* **2008**, *451*, 652–657. [[CrossRef](#)] [[PubMed](#)]
- Liao, M.; Wang, C.; Hong, Y.; Zhang, Y.; Cheng, X.; Sun, H.; Huang, X.; Ye, L.; Wu, J.; Shi, X.; et al. Industrial scale production of fibre batteries by a solution-extrusion method. *Nat. Nanotechnol.* **2022**, *17*, 372–377. [[CrossRef](#)] [[PubMed](#)]
- Chen, D.; Lou, Z.; Jiang, K.; Shen, G. Device configurations and future prospects of flexible/stretchable lithium-ion batteries. *Adv. Funct. Mater.* **2018**, *28*, 1805596. [[CrossRef](#)]
- Mackanic, D.G.; Kao, M.; Bao, Z. Enabling deformable and stretchable batteries. *Adv. Energy Mater.* **2020**, *10*, 2001424. [[CrossRef](#)]
- Sun, H.; Zhang, Y.; Zhang, J.; Sun, X.; Peng, H. Energy harvesting and storage in 1D devices. *Nat. Rev. Mater.* **2017**, *2*, 17023. [[CrossRef](#)]
- Zhang, P.; Wang, F.; Yu, M.; Zhuang, X.; Feng, X. Two-dimensional materials for miniaturized energy storage devices: From individual devices to smart integrated systems. *Chem. Soc. Rev.* **2018**, *47*, 7426–7451. [[CrossRef](#)]
- Ren, J.; Bai, W.; Guan, G.; Zhang, Y.; Peng, H. Flexible and weaveable capacitor wire based on a carbon nanocomposite fiber. *Adv. Mater.* **2013**, *25*, 5965–5970. [[CrossRef](#)]
- Kwon, Y.H.; Woo, S.-W.; Jung, H.-R.; Yu, H.K.; Kim, K.; Oh, B.H.; Ahn, S.; Lee, S.-Y.; Song, S.-W.; Cho, J.; et al. Cable-type flexible lithium ion battery based on hollow multi-helix electrodes. *Adv. Mater.* **2012**, *24*, 5192–5197. [[CrossRef](#)]
- Zhang, Y.; Bai, W.; Ren, J.; Weng, W.; Lin, H.; Zhang, Z.; Peng, H. Super-stretchy lithium-ion battery based on carbon nanotube fiber. *J. Mater. Chem. A* **2014**, *2*, 11054–11059. [[CrossRef](#)]

21. Zhang, L.; Huang, Y.; Zhang, Y.; Fan, W.; Liu, T. Three-dimensional nanoporous graphene–carbon nanotube hybrid frameworks for confinement of SnS<sub>2</sub> nanosheets: Flexible and binder-free papers with highly reversible lithium storage. *ACS Appl. Mater. Interfaces* **2015**, *7*, 27823–27830. [CrossRef] [PubMed]
22. Cai, J.; Jin, J.; Fan, Z.; Li, C.; Shi, Z.; Sun, J.; Liu, Z. 3D printing of a V<sub>8</sub>C<sub>7</sub>–VO<sub>2</sub> bifunctional scaffold as an effective polysulfide immobilizer and lithium stabilizer for Li–S batteries. *Adv. Mater.* **2020**, *32*, 2005967. [CrossRef] [PubMed]
23. Park, J.; Ahn, D.B.; Kim, J.; Cha, E.; Bae, B.-S.; Lee, S.-Y.; Park, J.-U. Printing of wirelessly rechargeable solid-state supercapacitors for soft, smart contact lenses with continuous operations. *Sci. Adv.* **2019**, *5*, eaay0764. [CrossRef] [PubMed]
24. Yan, Y.; Liu, X.; Yan, J.; Guan, C.; Wang, J. Electrospun nanofibers for new generation flexible energy storage. *Energy Environ. Mater.* **2021**, *4*, 502–521. [CrossRef]
25. Selvaraj, A.R.; Raja, I.S.; Chinnadurai, D.; Rajendiran, R.; Cho, I.; Han, D.-W.; Prabakar, K. Electrospun one dimensional (1D) pseudocapacitive nanorods embedded carbon nanofiber as positrode and graphene wrapped carbon nanofiber as negatrode for enhanced electrochemical energy storage. *J. Energy Storage* **2022**, *46*, 103731. [CrossRef]
26. Cheng, Y.; Wang, K.; Qi, Y.; Liu, Z. Chemical vapor deposition method for graphene fiber materials. *Acta Phys.-Chim. Sin.* **2020**, *38*, 2006046. [CrossRef]
27. Sun, C.; Chen, S.; Li, Z. Controllable synthesis of Fe<sub>2</sub>O<sub>3</sub>-carbon fiber composites via a facile sol-gel route as anode materials for lithium ion batteries. *Appl. Surf. Sci.* **2018**, *427*, 476–484. [CrossRef]
28. Wang, Y.; Chen, C.; Xie, H.; Gao, T.; Yao, Y.; Pastel, G.; Han, X.; Li, Y.; Zhao, J.; Fu, K.; et al. 3D-printed all-fiber li-ion battery toward wearable energy storage. *Adv. Funct. Mater.* **2017**, *27*, 1703140. [CrossRef]
29. Praveen, S.; Sim, G.S.; Ho, C.W.; Lee, C.W. 3D-printed twisted yarn-type Li-ion battery towards smart fabrics. *Energy Storage Mater.* **2021**, *41*, 748–757. [CrossRef]
30. De Castro Motta, J.; Qaderi, S.; Farina, I.; Singh, N.; Amendola, A.; Fraternali, F. Experimental characterization and mechanical modeling of additively manufactured TPU components of innovative seismic isolators. *Acta Mech.* **2022**, *1*–12. [CrossRef]
31. Buchanan, C.; Gardner, L. Metal 3D printing in construction: A review of methods, research, applications, opportunities and challenges. *Eng. Struct.* **2019**, *180*, 332–348. [CrossRef]
32. Zhu, C.; Liu, T.; Qian, F.; Chen, W.; Chandrasekaran, S.; Yao, B.; Song, Y.; Duoss, E.B.; Kuntz, J.D.; Spadaccini, C.M.; et al. 3D printed functional nanomaterials for electrochemical energy storage. *Nano Today* **2017**, *15*, 107–120. [CrossRef]
33. Zhang, F.; Wei, M.; Viswanathan, V.V.; Swart, B.; Shao, Y.; Wu, G.; Zhou, C. 3D printing technologies for electrochemical energy storage. *Nano Energy* **2017**, *40*, 418–431. [CrossRef]
34. Sousa, R.E.; Costa, C.M.; Lanceros-Méndez, S. Advances and future challenges in printed batteries. *ChemSusChem* **2015**, *8*, 3539–3555. [CrossRef] [PubMed]
35. Tian, X.; Jin, J.; Yuan, S.; Chua, C.K.; Tor, S.B.; Zhou, K. Emerging 3D-printed electrochemical energy storage devices: A critical review. *Adv. Energy Mater.* **2017**, *7*, 1700127. [CrossRef]
36. Pei, M.; Shi, H.; Yao, F.; Liang, S.; Xu, Z.; Pei, X.; Wang, S.; Hu, Y. 3D printing of advanced lithium batteries: A designing strategy of electrode/electrolyte architectures. *J. Mater. Chem. A* **2021**, *9*, 25237–25257. [CrossRef]
37. Truby, R.L.; Lewis, J.A. Printing soft matter in three dimensions. *Nature* **2016**, *540*, 371–378. [CrossRef]
38. Wang, L.-C.; Song, W.-L.; Fang, D. Twistable Origami and Kirigami: From structure-guided smartness to mechanical energy storage. *ACS Appl. Mater. Interfaces* **2019**, *11*, 3450–3458. [CrossRef]
39. Rocha, V.G.; Saiz, E.; Tirichenko, I.S.; García-Tuñón, E. Direct ink writing advances in multi-material structures for a sustainable future. *J. Mater. Chem. A* **2020**, *8*, 15646–15657. [CrossRef]
40. Mohammadpourfazeli, S.; Arash, S.; Ansari, A.; Yang, S.; Mallick, K.; Bagherzadeh, R. Future prospects and recent developments of polyvinylidene fluoride (PVDF) piezoelectric polymer; fabrication methods, structure, and electro-mechanical properties. *RSC Adv.* **2023**, *13*, 370–387. [CrossRef]
41. Houis, S.; Engelhardt, E.M.; Wurm, F.; Gries, T. Application of polyvinylidene fluoride (PVDF) as a biomaterial in medical textiles. *Med. Healthc. Text.* **2010**, *342*–352. [CrossRef]
42. Liao, C.; Li, Y.; Tjong, S.C. Graphene nanomaterials: Synthesis, biocompatibility, and cytotoxicity. *Int. J. Mol. Sci.* **2018**, *19*, 3564. [CrossRef] [PubMed]
43. Trück, J.; Wang, P.; Buch, E.; Groos, J.; Niesen, S.; Buchmeiser, M.R. Communication—Lithium titanate as mg-ion insertion anode for mg-ion sulfur batteries based on sulfurated poly(acrylonitrile) composite. *J. Electrochem. Soc.* **2022**, *169*, 010505. [CrossRef]
44. Carvalho, D.V.; Loeffler, N.; Kim, G.-T.; Marinaro, M.; Wohlfahrt-Mehrens, M.; Passerini, S. Study of water-based lithium titanate electrode processing: The role of pH and binder molecular structure. *Polymers* **2016**, *8*, 276. [CrossRef]
45. Pei, S.; Cheng, H.-M. The reduction of graphene oxide. *Carbon* **2012**, *50*, 3210–3228. [CrossRef]
46. Tao, R.; Li, F.; Lu, X.; Liu, F.; Xu, J.; Kong, D.; Zhang, C.; Tan, X.; Ma, S.; Shi, W.; et al. High-conductivity–dispersibility graphene made by catalytic exfoliation of graphite for lithium-ion battery. *Adv. Funct. Mater.* **2021**, *31*, 2007630. [CrossRef]
47. Wang, P.; Ye, Y.; Liang, D.; Sun, H.; Liu, J.; Tian, Z.; Liang, C. Layered mesoporous Mg(OH)<sub>2</sub>/GO nanosheet composite for efficient removal of water contaminants. *RSC Adv.* **2016**, *6*, 26977–26983. [CrossRef]
48. Zhang, D.; Chi, B.; Li, B.; Gao, Z.; Du, Y.; Guo, J.; Wei, J. Fabrication of highly conductive graphene flexible circuits by 3D printing. *Synth. Met.* **2016**, *217*, 79–86. [CrossRef]
49. Gómez-Navarro, C.; Weitz, R.T.; Bittner, A.M.; Scolari, M.; Mews, A.; Burghard, M.; Kern, K. Electronic transport properties of individual chemically reduced graphene oxide sheets. *Nano Lett.* **2007**, *7*, 3499–3503. [CrossRef]

50. De Silva, K.K.H.; Huang, H.-H.; Yoshimura, M. Progress of reduction of graphene oxide by ascorbic acid. *Appl. Surf. Sci.* **2018**, *447*, 338–346. [[CrossRef](#)]
51. Stankovich, S.; Dikin, D.A.; Domke, G.H.B.; Kohlhaas, K.M.; Zimney, E.J.; Stach, E.A.; Piner, R.D.; Nguyen, S.T.; Ruoff, R.S. Graphene-based composite materials. *Nature* **2006**, *442*, 282–286. [[CrossRef](#)] [[PubMed](#)]
52. Spinelli, G.; Lamberti, P.; Tucci, V.; Ivanova, R.; Tabakova, S.; Ivanov, E.; Kotsilkova, R.; Cimmino, S.; Di Maio, R.; Silvestre, C. Rheological and electrical behaviour of nanocarbon/poly(lactic) acid for 3D printing applications. *Compos. Part B Eng.* **2019**, *167*, 467–476. [[CrossRef](#)]
53. Ponnamma, D.; Sadasivuni, K.K.; Cabibihan, J.-J.; Yoon, W.J.; Kumar, B. Reduced graphene oxide filled poly(dimethyl siloxane) based transparent stretchable, and touch-responsive sensors. *Appl. Phys. Lett.* **2016**, *108*, 171906. [[CrossRef](#)]
54. Mo, R.; Lei, Z.; Sun, K.; Rooney, D. Facile Synthesis of anataseTiO<sub>2</sub> quantum-dot/graphene-nanosheet composites with enhanced electrochemical performance for lithium-ion batteries. *Adv. Mater.* **2014**, *26*, 2084–2088. [[CrossRef](#)]
55. Mo, R.; Li, F.; Tan, X.; Xu, P.; Tao, R.; Shen, G.; Lu, X.; Liu, F.; Shen, L.; Xu, B.; et al. High-quality mesoporous graphene particles as high-energy and fast-charging anodes for lithium-ion batteries. *Nat. Commun.* **2019**, *10*, 1474. [[CrossRef](#)]
56. Lee, C.; Wei, X.; Kysar, J.W.; Hone, J. Measurement of the elastic properties and intrinsic strength of monolayer graphene. *Science* **2008**, *321*, 385–388. [[CrossRef](#)]
57. Qaderi, S.; Ebrahimi, F. Vibration analysis of polymer composite plates reinforced with graphene platelets resting on two-parameter viscoelastic foundation. *Eng. Comput.* **2022**, *38*, 419–435. [[CrossRef](#)]
58. Seyssieq, I.; Ferrasse, J.-H.; Roche, N. State-of-the-art: Rheological characterisation of wastewater treatment sludge. *Biochem. Eng. J.* **2003**, *16*, 41–56. [[CrossRef](#)]
59. Lewis, J.A. Direct ink writing of 3D functional materials. *Adv. Funct. Mater.* **2006**, *16*, 2193–2204. [[CrossRef](#)]
60. Clausen, A.; Wang, F.; Jensen, J.S.; Sigmund, O.; Lewis, J.A. Topology optimized architectures with programmable poisson's ratio over large deformations. *Adv. Mater.* **2015**, *27*, 5523–5527. [[CrossRef](#)]
61. Fathy, M.; Gomaa, A.; Taher, F.A.; El-Fass, M.M.; Kashyout, A.E.-H.B. Optimizing the preparation parameters of GO and rGO for large-scale production. *J. Mater. Sci.* **2016**, *51*, 5664–5675. [[CrossRef](#)]
62. Hao, Z.; Zhang, Q.; Xu, X.; Zhao, Q.; Wu, C.; Liu, J.; Wang, H. Nanochannels regulating ionic transport for boosting electrochemical energy storage and conversion: A review. *Nanoscale* **2020**, *12*, 15923–15943. [[CrossRef](#)] [[PubMed](#)]
63. Yang, J.; Duan, X.; Guo, W.; Li, D.; Zhang, H.; Zheng, W. Electrochemical performances investigation of NiS/rGO composite as electrode material for supercapacitors. *Nano Energy* **2014**, *5*, 74–81. [[CrossRef](#)]
64. Zhang, W.; Tu, Z.; Qian, J.; Choudhury, S.; Archer, L.A.; Lu, Y. Design Principles of functional polymer separators for high-energy, metal-based batteries. *Small* **2018**, *14*, 1703001. [[CrossRef](#)]
65. Wu, Z.-S.; Ren, W.; Xu, L.; Li, F.; Cheng, H.-M. Doped graphene sheets as anode materials with superhigh rate and large capacity for lithium ion batteries. *ACS Nano* **2011**, *5*, 5463–5471. [[CrossRef](#)]
66. Cheng, Q.; Song, Z.; Ma, T.; Smith, B.B.; Tang, R.; Yu, H.; Jiang, H.; Chan, C.K. Folding paper-based lithium-ion batteries for higher areal energy densities. *Nano Lett.* **2013**, *13*, 4969–4974. [[CrossRef](#)]
67. Tan, X.; Mo, R.; Xu, J.; Li, X.; Yin, Q.; Shen, L.; Lu, Y. High performance sodium ion anodes based on Sn<sub>4</sub>P<sub>3</sub> encapsulated within amphiphilic graphene tubes. *Adv. Energy Mater.* **2022**, *12*, 2102345. [[CrossRef](#)]

**Disclaimer/Publisher's Note:** The statements, opinions and data contained in all publications are solely those of the individual author(s) and contributor(s) and not of MDPI and/or the editor(s). MDPI and/or the editor(s) disclaim responsibility for any injury to people or property resulting from any ideas, methods, instructions or products referred to in the content.